The Knee 26 (2019) 339–346

Contents lists available at ScienceDirect

The Knee

Strain distribution of the anterolateral ligament during internal rotation at different knee flexion angles: A biomechanical study on human cadavers

Yibei Wang, Shiqi Li, Daorong Xu, Lei Qian, Chunyu Jiang, Maoqing Fu, Peidong Sun, Jun Ouyang *

Department of Anatomy, Guangdong Provincial Key Laboratory of Medical Biomechanics, Southern Medical University, Guangzhou 510515, China

ARTICLE INFO

Article history:
Received 10 May 2018
Received in revised form 19 October 2018
Accepted 8 January 2019

Keywords:
Anterolateral ligament
Internal rotation
Strain
Digital image correlation
Knee biomechanics

ABSTRACT

Background: Injuries of the anterolateral ligament (ALL) are fairly common in patients with ruptures of the anterior cruciate ligament (ACL). Before considering repair or reconstruction of the ALL, the lack of knowledge with regard to the biomechanical behavior of this ligament must be considered. The purpose of this study was to analyze the strain of the ALL induced by tibial internal rotation at different flexion angles and find out the strain distribution features.

Methods: The ALLs of ten fresh-frozen cadaver knees were dissected. All specimens underwent tibial internal rotation from 0° to 25° at 30°, 60°, 90°, and 120° of knee flexion. Strain distribution of the ALL during internal rotation was recorded by digital image correlation (DIC). The overall strain and sub-regional strain were measured.

Results: The strain of the ALL increased with increasing tibial internal rotation. With 25° of internal rotation, the overall strain at each flexion angle was 12.89 ± 2.73% (30°), 15.32 ± 2.50% (60°), 18.94 ± 2.34% (90°), and 20.10 ± 3.27% (120°). The sub-regional strain was significantly different at all flexion angles. The strain of the distal 1/3 of the ALL was the greatest, followed by the middle 1/3, while the proximal 1/3 was the smallest (all $P < 0.001$).

Conclusion: The ALL resisted internal rotation of the tibia by becoming more tense with increasing rotation. A significantly high strain was observed in the distal portion near the tibial insertion site of the ALL, which may suggest that this region is prone to injury with excessive internal rotation.

1. Introduction

Recent investigations have revealed that injuries of the anterolateral ligament (ALL) are fairly common in patients with ruptures of the anterior cruciate ligament (ACL) [1–4]. With regard to a high degree of knee rotational instability or a high risk of graft re-rupture, some authors have suggested that with combined injuries to the ACL and ALL, reconstruction of both ligaments should be considered to better restore knee stability [5,6].

Before considering ALL reconstruction, greater knowledge of the biomechanical characteristics may help in understanding the in vivo behavior and function of this ligament. There is a growing body of research into the mechanical behavior of the ALL. Some authors have studied the length changes of the ALL during various knee motions [7–9]. In addition, through comparisons of the forces in the ligaments, Parsons et al. found that the contribution of the ALL during internal rotation increased significantly with

* Corresponding author at: Department of Anatomy, Southern Medical University, No.1063 Shatainan Road, Baiyun District, Guangzhou, Guangdong 510515, China.
E-mail address: jouyang@126.com. (J. Ouyang).

https://doi.org/10.1016/j.knee.2019.01.001
0968-0160/

increasing flexion [10]. However, there is a lack of studies researching the detailed strain on the ALL during knee motion. Drews et al. used a sensor device to measure the strain on the ALL during knee motion [11]. The strain they calculated was the elongation of a sensor that was glued onto the ALL. Corbo et al. found that there were differences in the sub-regional tensile properties of the ALL [12]. In consideration of the non-uniform tensile properties of the ALL, sub-regional strain on the ALL may be different during passive knee motion. Therefore, considering the partial elongation of the sensors to be equivalent to the strain on the whole ALL may be inappropriate and less accurate. Because the sensors require some form of fixation to the tissue, measurement errors may be introduced. More importantly, the sensor acts as a point gauge and thus fails to display regional strain patterns.

This study aimed to analyze the strain distribution of the ALL induced by tibial internal rotation at different knee flexion angles using digital image correlation (DIC). Furthermore, sub-regional strain on the ALL was analyzed and compared to investigate which region of this ligament has the greatest strain. High strain on a region may indicate that this region is prone to injury. The hypothesis of this study was that the ALL might exhibit unique patterns of strain distribution in response to tibial internal rotation.

2. Material and methods

Ten fresh-frozen cadaveric knees (six male, four female; seven left, three right knees) with an average age of 52 years (range from 36 to 66 years) were donated. Ethical approval was obtained from the ethics committee of Southern Medical University. All subjects had provided written informed consent confirming their intent to donate their bodies for medical research purposes. Combining the medical history of the donors and the results of fluoroscopy, all specimens were without evidence of prior knee injury, surgery, arthritis, or anatomical abnormality. The femur was cut 20 cm proximal to the joint line, while the tibia was cut 20 cm distal to the joint line. The fibula was cut five centimeters shorter than the tibia. The specimens were stored at −20 °C and thawed at room temperature for 24 h before dissection.

2.1. Specimen preparation

All specimens were dissected by the same surgeon. The specimens were kept moist with saline solution during the entire preparation. The dissection was realized following the protocol defined by Claes et al. [13]. All musculature except the popliteal muscle–tendon complex was removed, while the ligaments and posterior capsular restraints were left in place. After defining the area of the ALL along the distribution of the fibers and fully exposing it (Figure 1), both diaphyseal ends of the femur and tibia were potted in polymethylmethacrylate, while the fibula was distally fixed to the tibia using a bicortical screw to maintain stabilization.

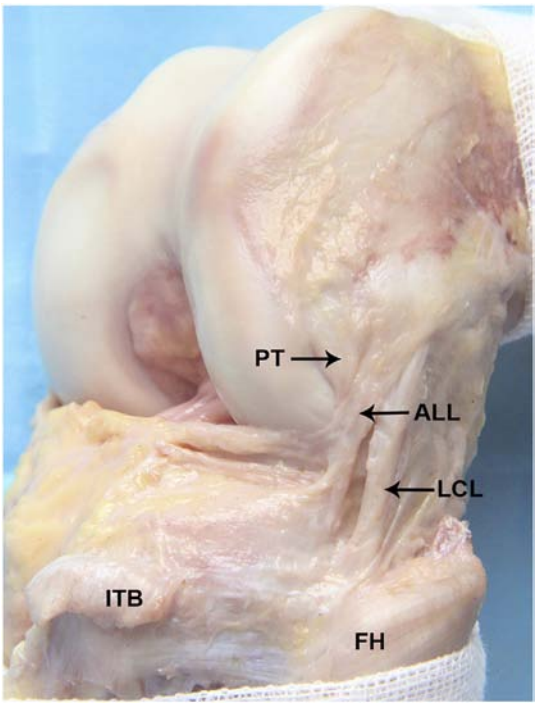

Figure 1. Lateral view of a left knee with internal rotation: the anterolateral ligament (ALL) is divided from the lateral collateral ligament (LCL) and popliteus tendon (PT). The iliotibial band (ITB) and fibula head (FH) are also highlighted.

2.2. Mechanical loading

The specimens were mounted on the testing apparatus (ElectroForce3510-AT, Bose Corp., USA) through a specifically designed rig, which allowed flexion/extension and external or internal rotation of the tibia (Figure 2). The position of the femur was controlled by the two slide tracks of the rig and the load arm. The tibia was mounted on the torque motor. The flexion angle of the knee was defined by a Motion Capture system (Raptor-4, Motion Analysis Corp., USA) through markers that were glued on to the anatomical landmarks. Based on the anatomical landmarks, a coordinate system was defined using methods previously reported [14,15]. The specimen was initially subjected to a vertical load of 30 N to ensure tibiofemoral contact [11].

Before testing, the specimens were preloaded with internal rotation to 25° at 90° of flexion 10 times to prevent soft tissue hysteresis. To simulate the strain on the ALL induced by internal rotation of the tibia, at four positions of flexion (30°, 60°, 90°, and 120°), the tibia was loaded with internal torque at a rate of two degrees per second until 25° of rotation was reached. The rotational process was performed three times at each flexion angle, and the average data was used for analysis. During the test, there was no tear in the ALL or in other ligaments.

2.3. Strain measurement

The strain on the ALL was recorded by a non-contact optical three-dimensional measuring system (ARAMIS 4M, GOM Corp., Germany) using DIC as previously reported [16,17]. Image recognition was performed by two digital cameras to analyze and compare the digital images acquired from the surface of a substrate instead of surface markers. By tracing a randomly applied high-contrast speckle pattern using white light, displacement and strain within the specimen were calculated from the images. To obtain an optimal contrast ratio, the ALL was dyed dark blue by methylene, and subsequently sprayed with water-based white paint on the surface. This dyeing method does not alter the mechanical properties of the ligament [18]. The initial imaging process defined unique correlation areas known as macro-image facets, typically consisting of a square of 15 pixels across the entire imaging area. Each facet was a measurement point, or 'extensometer point' and 'strain rosette'. These measured facets were tracked in each successive image, and the strain on the ligament surface was calculated by comparing the digital images of the knee with internal rotation with those without rotation at different flexion angles. To maximize successive facets and minimize missing measurements in this study, with our repeated measurement, the resolution of the images was 2358 × 1728 pixels, the measuring

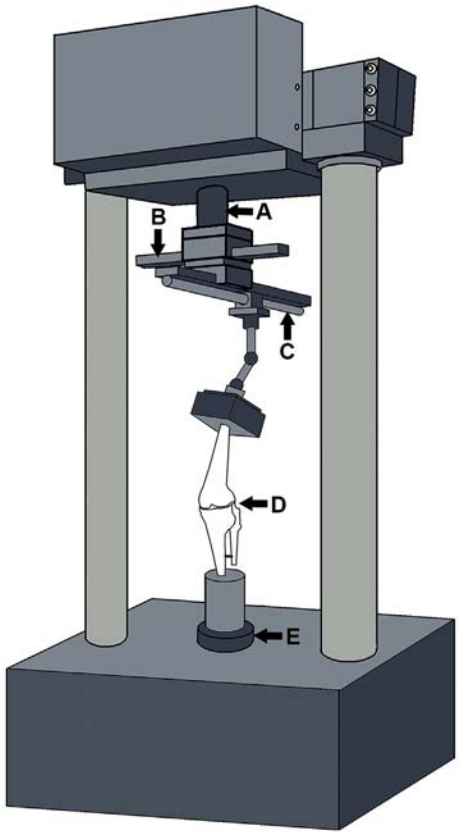

Figure 2. Schematic of the specimen mounted on the testing apparatus through a specifically designed rig. (A) Load arm; (B) slide track of horizontal axis; (C) slide track of sagittal axis; (D) knee specimen; (E) torque motor.

volume was set at 65 × 48 mm; the frequency of exposure was set at four hertz, and the time of exposure was set between 65 and 95 ms. An adequate depth of aperture dependent of field, 22–36 mm, was obtained by setting the *F* value between 16 and 22 mm. The accuracy of the strain measurement was 0.005%. The strain analyzed was the average value of major principal strain on the area designated [16,17].

To analyze the strain distribution features in the ALL, along the longitudinal axis of the ligament, the ALL was divided into three portions: the proximal third (near the femoral origin), middle third, and distal third (near the tibial insertion).

2.4. Statistical analysis

SPSS software (v. 21.0; IBM Corp., USA) was used for statistical analysis. Normal distribution of data was confirmed using a Shapiro–Wilk test, and the homogeneity of variances was verified using Levene's test. The strain was presented as mean ± standard deviation (SD). With the largest internal rotation angle (25°), sub-regional strain in different portions was compared using one-way analysis of variance (ANOVA) with Tukey post hoc testing. These comparisons were performed at each flexion angle (30°, 60°, 90°, and 120°). For all comparisons, the level of significance was set at $P < 0.05$.

3. Results

3.1. Overall strain

An example of cloud maps of the ALL strain distribution during tibial internal rotation can be seen in Figure 3. The ALL became more tense with increasing internal rotation. Trend curves of overall strain on the ALL during internal rotation at each flexion angle are shown in Figure 4. With 25° of internal rotation, the overall strain and sub-regional strain at each flexion angle are shown in Table 1.

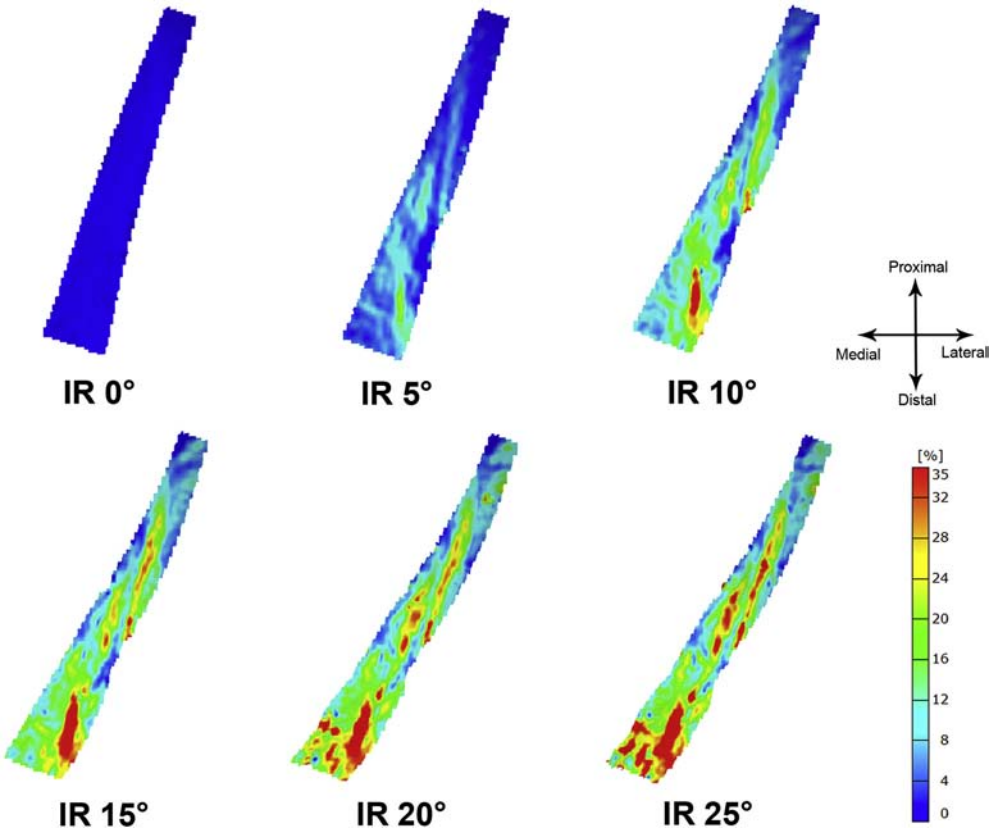

Figure 3. Cloud maps of strain distribution of the anterolateral ligament (ALL) during tibial internal rotation (IR) at 90° of knee flexion, with maximizing strain represented by a color change from blue to red.

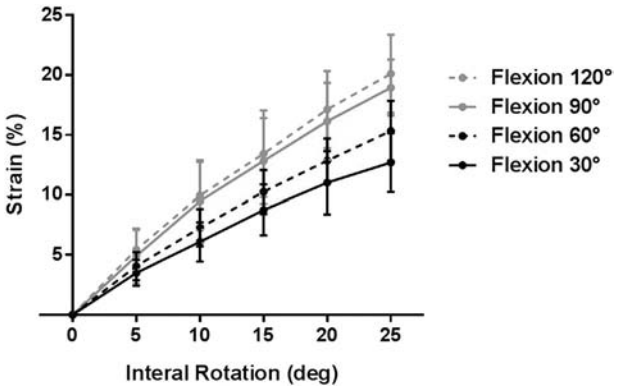

Figure 4. Trend curves of overall strain (mean ± standard deviation) of the anterolateral ligament (ALL) during tibial internal rotation (IR) at different knee flexion angles.

3.2. Sub-regional strain

An example of digital image of ALL sub-regional strain is shown in Figure 5. With 25° of internal rotation, the sub-regional strain was significantly different at all flexion angles (all $P < 0.001$). The strain on the distal third of the ALL was the greatest, followed by the middle third, while the proximal third was the smallest (all $P < 0.001$) (Figure 6). Figure 5 also shows that the region with high strain is mainly located at distal portion near the tibial insertion site.

4. Discussion

The aims of this study were to characterize the mechanical behavior of the ALL in response to tibial internal rotations, which were intended to simulate physiologically and clinically relevant conditions where function, injury, and repair of the ALL are implicated. The findings of this study have shown that the ALL resisted the internal rotation of the tibia by becoming more tense with increasing internal rotation. More importantly, a significantly high strain was observed in the distal portion near the tibial insertion site of the ALL.

High strain on the distal portion of the ALL may suggest that this region is at risk of injury with excessive internal rotation. Most imaging studies have reported that a high rate of lesions was found in the distal portion of the ALL [1,2,4,19]. Claes et al. observed that the majority of ALL abnormalities (77.8%) were situated in the distal part of the ligament [1]. Van Dyck et al. suggested that injuries of the ALL might be caused by excessive internal tibial torque, and 71% of ALL lesions were found in the distal component with 37% being bony avulsions or Segond fractures [2]. In addition, an ultrasonography study by Faruch Bilfeld et al. showed that 78.9% of ALL lesions were located at the tibial attachment [4]. However, Helito et al. reported the same rate (45.4%) of lesions in the proximal and distal portions of the ALL [3]. The disparate mechanisms of injury, which are the most important factors that predict structural abnormalities, may account for the variable results of previous studies [20].

The high strain on the distal part of the ALL may be due to the relatively large tensile stress of this region. Corbo et al. found the differences in the sub-regional tensile properties of the ALL: the ALL below the meniscus was significantly stronger and stiffer when compared with the ALL above the meniscus [12]. Limited differences in the histological results were found between the two ALL sections, indicating that the two sections have the same morphological characteristics. Therefore, they inferred that the differences in the infra-meniscal and supra-meniscal tensile properties may be due to the supra-meniscal fibers not being subjected to the same load magnitude as the infra-meniscal sections during normal loading scenarios. This corresponds with our inference based on the different strains of the various regions of the ALL.

The stress distribution in the ligament is closely related to the direction of the applied load. A tensile test of the human ACL revealed that the tensile stress distribution in the ligament was consistent when tested along the anatomical axis of the ACL,

Table 1
The overall and sub-regional strain (mean ± standard deviation) of the anterolateral ligament with 25° of tibial internal rotation at different knee flexion angles.

Flexion	Overall strain (%)	Sub-regional strain (%)		
		Proximal third	Middle third	Distal third
30°	12.89 ± 2.73	5.06 ± 2.32	12.46 ± 3.69[b]	19.04 ± 3.69[a]
60°	15.32 ± 2.50	6.53 ± 2.51	15.01 ± 2.75[b]	21.93 ± 3.20[a]
90°	18.94 ± 2.34	9.93 ± 2.64	17.84 ± 2.76[b]	26.23 ± 4.26[a]
120°	20.10 ± 3.27	9.68 ± 3.12	17.84 ± 3.17[b]	27.96 ± 4.51[a]

[a] Significantly different from the middle third ($P < 0.001$) and proximal third ($P < 0.001$).
[b] Significantly different from the proximal third ($P < 0.001$).

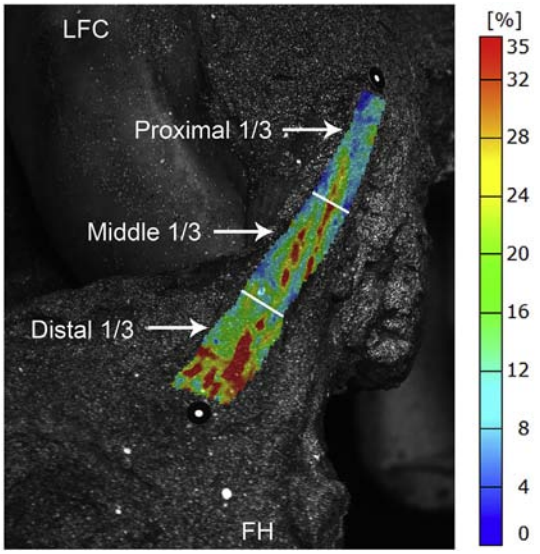

Figure 5. Digital image of sub-regional strain on the anterolateral ligament (ALL) with 25° of tibial internal rotation (IR) at 90° of knee flexion: A colorful strain map of the area under study is superimposed on to the ALL, with maximizing strain represented by a color change from blue to red. The ALL was divided into three portions: proximal third, middle third, distal third. Lateral femoral condyle (LFC) and fibula head (FH) are highlighted.

though the tensile stress distribution in the ACL was not uniform when tested along the tibial axis [21]. In our study, the direction of load exerted on the ALL, conducted through internal rotation of the tibia, was not along the anatomical axis of the ALL. Therefore, when internal torque is applied on the tibia, the tensile stress of the distal part of ALL may be the greatest. If the stress increases beyond the upper limit of the physiological range of distal ALL, but not beyond the failure load magnitude of the tibia near the insertion site, it will cause the distal portion to fail. If osteoporosis occurs, it may cause the Segond fracture, which may represent a bony avulsion of the ALL as indicated by previous studies [22–24]. In consideration of these cases, with regard to ALL repair or reconstruction, we suggested that the distal portion of the ligament and the fixation on the tibia need reinforcement to reduce the re-injury risk.

The ALL resisted internal rotation of the tibia by becoming more tense with increasing rotation. The strain in this study is much lower than the ultimate ALL strain at failure (36.0 ± 4.5%; 37.8 ± 7.9%) that other studies reported [25,26]. Zens et al. found that the length changes of the ALL with internal rotation were greater at high-flexion angles, and suggested that the ALL can be considered a stabilizer against internal rotation of the tibia, especially at high-flexion angles of the knee [8]. Our results also show the similar trend that strain on the ALL induced by tibial internal rotation tends to be greater at high-flexion angles (90° and 120°) of the knee. A study by Parsons et al. also revealed that the ALL has a different stabilizing effect at different knee flexion angles [10].

In this study, three-dimensional DIC was adopted to investigate the strain distribution of the ALL. DIC was successfully utilized in several studies on bones [16,27], tendons [28], ligaments [17,18,29], and other biological soft tissues [30,31], in which deformation with a full field was determined, and the high strain region could be distinguished. DIC is a non-contact, flexible optical method for strain measurement that has been frequently used in determinations of the mechanical properties of biological materials. As a strain measurement method, DIC has many advantages, including some of that make it optimal for biomedical studies of soft tissues. First, many soft tissues undergo moderate deformation in vivo, which may exceed the range of measurement available

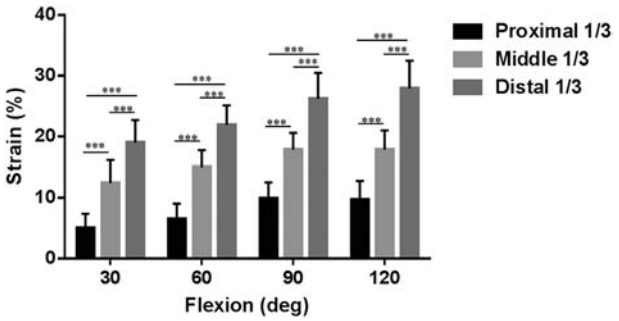

Figure 6. Strain (mean ± standard deviation) of different portions of the anterolateral ligament (ALL) with 25° of tibial internal rotation (IR) at different knee flexion angles (***$P < 0.001$).

from interferometric techniques [32]. Compared with the contact measuring method, DIC has a much greater range of measurement. Second, the non-contact measuring characteristic of DIC, a major advantage for measuring strain on the soft tissues, could minimize the effects of reinforcement and/or modification in biological material response. Third, as a full field measurement method, DIC provides information not only for the average response in the imaged region, but also for the local variations in response that are important when studying non-homogeneous materials such as ligamentous tissues [30].

This study had several limitations. First, in order to visualize the ALL, it was necessary to dissect the iliotibial band (ITB) even though the ITB plays an important role in controlling internal rotation [33,34]. This may have an effect on the actual strain behavior of the ALL. Second, the ligament might become fatigued with repeated motor-controlled passive rotation. It is possible that the magnitude of the stain seen on the ALL may be different from that in a dynamic in vivo condition. However, we believe that the variation trend and distribution pattern of strain are consistent on account of the support of previous studies [1,2,4,8,10,12,19]. Third, we only studied the strain on the ALL induced by tibial internal rotation, because several studies have found that the ALL became tense with internal rotation but slackened with external rotation [13,23,35]. Strain on the ALL induced by other modes of knee motion needs further study.

5. Conclusion

This study analyzed the strain on the ALL induced by tibial internal rotation at different flexion angles and revealed the strain distribution features. The ALL resisted the internal rotation of the tibia by becoming more tense with increasing rotation. A significantly high strain was observed in the distal portion near the tibial insertion site of the ALL, which may suggest that this region is prone to injury with excessive internal rotation. The identification of regions under high strain has potential implications for ALL repair or reconstruction techniques to reduce the re-injury risk.

Conflict of interest

The authors have no conflicts of interest to declare.

References

[1] Claes S, Bartholomeeusen S, Bellemans J. High prevalence of anterolateral ligament abnormalities in magnetic resonance images of anterior cruciate ligament-injured knees. Acta Orthop Belg 2014;80:45–9.
[2] Van Dyck P, Clockaerts S, Vanhoenacker FM, Lambrecht V, Wouters K, De Smet E, et al. Anterolateral ligament abnormalities in patients with acute anterior cruciate ligament rupture are associated with lateral meniscal and osseous injuries. Eur Radiol 2016;26:3383–91.
[3] Helito CP, Helito PVP, Leao RV, Demange MK, Bordalo-Rodrigues M. Anterolateral ligament abnormalities are associated with peripheral ligament and osseous injuries in acute ruptures of the anterior cruciate ligament. Knee Surg Sports Traumatol Arthrosc 2017;25:1140–8.
[4] Faruch Bilfeld M, Cavaignac E, Wytrykowski K, Constans O, Lapegue F, Chiavassa Gandois H, et al. Anterolateral ligament injuries in knees with an anterior cruciate ligament tear: contribution of ultrasonography and MRI. Eur Radiol 2018;28:58–65.
[5] Nitri M, Rasmussen MT, Williams BT, Moulton SG, Cruz RS, Dornan GJ, et al. An in vitro robotic assessment of the anterolateral ligament, part 2: anterolateral ligament reconstruction combined with anterior cruciate ligament reconstruction. Am J Sports Med 2016;44:593–601.
[6] Sonnery-Cottet B, Saithna A, Cavalier M, Kajetanek C, Temponi EF, Daggett M, et al. Anterolateral ligament reconstruction is associated with significantly reduced ACL graft rupture rates at a minimum follow-up of 2 years: a prospective comparative study of 502 patients from the SANTI study group. Am J Sports Med 2017;45:1547–57.
[7] Imbert P, Lutz C, Daggett M, Niglis L, Freychet B, Dalmay F, et al. Isometric characteristics of the anterolateral ligament of the knee: a cadaveric navigation study. Art Ther 2016;32:2017–24.
[8] Zens M, Niemeyer P, Ruhhammer J, Bernstein A, Woias P, Mayr HO, et al. Length changes of the anterolateral ligament during passive knee motion: a human cadaveric study. Am J Sports Med 2015;43:2545–52.
[9] Neri T, Palpacuer F, Testa R, Bergandi F, Boyer B, Farizon F, et al. The anterolateral ligament: anatomic implications for its reconstruction. Knee 2017;24:1083–9.
[10] Parsons EM, Gee AO, Spiekerman C, Cavanagh PR. The biomechanical function of the anterolateral ligament of the knee. Am J Sports Med 2015;43:669–74.
[11] Drews BH, Kessler O, Franz W, Durselen L, Freutel M. Function and strain of the anterolateral ligament part i: biomechanical analysis. Knee Surg Sports Traumatol Arthrosc 2017;25:1132–9.
[12] Corbo G, Norris M, Getgood A, Burkhart TA. The infra-meniscal fibers of the anterolateral ligament are stronger and stiffer than the supra-meniscal fibers despite similar histological characteristics. Knee Surg Sports Traumatol Arthrosc 2017;25:1078–85.
[13] Claes S, Vereecke E, Maes M, Victor J, Verdonk P, Bellemans J. Anatomy of the anterolateral ligament of the knee. J Anat 2013;223:321–8.
[14] Imhauser C, Mauro C, Choi D, Rosenberg E, Mathew S, Nguyen J, et al. Abnormal tibiofemoral contact stress and its association with altered kinematics after center–center anterior cruciate ligament reconstruction: an in vitro study. Am J Sports Med 2013;41:815–25.
[15] Thein R, Boorman-Padgett J, Stone K, Wickiewicz TL, Imhauser CW, Pearle AD. Biomechanical assessment of the anterolateral ligament of the knee: a secondary restraint in simulated tests of the pivot shift and of anterior stability. J Bone Joint Surg Am 2016;98:937–43.
[16] Ali AM, Newman SDS, Hooper PA, Davies CM, Cobb JP. The effect of implant position on bone strain following lateral unicompartmental knee arthroplasty: a biomechanical model using digital image correlation. Bone Joint Res 2017;6:522–9.
[17] Xu D, Wang Y, Jiang C, Fu M, Li S, Qian L, et al. Strain distribution in the anterior inferior tibiofibular ligament, posterior inferior tibiofibular ligament, and interosseous membrane using digital image correlation. Foot Ankle Int 2018;39:618–28.
[18] Luyckx T, Verstraete M, De Roo K, Van Der Straeten C, Victor J. High strains near femoral insertion site of the superficial medial collateral ligament of the knee can explain the clinical failure pattern. J Orthop Res 2016;34:2016–24.
[19] Kosy JD, Schranz PJ, Patel A, Anaspure R, Mandalia VI. The magnetic resonance imaging appearance of the anterolateral ligament of the knee in association with anterior cruciate rupture. Skeletal Radiol 2017;46:1193–200.
[20] MacMahon PJ, Palmer WE. A biomechanical approach to MRI of acute knee injuries. AJR Am J Roentgenol 2011;197:568–77.
[21] Woo SL, Hollis JM, Adams DJ, Lyon RM, Takai S. Tensile properties of the human femur-anterior cruciate ligament-tibia complex. The effects of specimen age and orientation. Am J Sports Med 1991;19:217–25.
[22] Claes S, Luyckx T, Vereecke E, Bellemans J. The segond fracture: a bony injury of the anterolateral ligament of the knee. Art Ther 2014;30:1475–82.
[23] Dodds AL, Halewood C, Gupte CM, Williams A, Amis AA. The anterolateral ligament: anatomy, length changes and association with the segond fracture. Bone Joint J 2014;96-B:325–31.

[24] Porrino Jr J, Maloney E, Richardson M, Mulcahy H, Ha A, Chew FS. The anterolateral ligament of the knee: MRI appearance, association with the segond fracture, and historical perspective. AJR Am J Roentgenol 2015;204:367–73.
[25] Zens M, Feucht MJ, Ruhhammer J, Bernstein A, Mayr HO, Sudkamp NP, et al. Mechanical tensile properties of the anterolateral ligament. J Exp Orthop 2015;2:7.
[26] Smeets K, Slane J, Scheys L, Forsyth R, Claes S, Bellemans J. The anterolateral ligament has similar biomechanical and histologic properties to the inferior glenohumeral ligament. Art Ther 2017;33:1028–35 [e1].
[27] Tayton E, Evans S, O'Doherty D. Mapping the strain distribution on the proximal femur with titanium and flexible-stemmed implants using digital image correlation. J Bone Joint Surg Br 2010;92:1176–81.
[28] von der Heide N, Ebneter L, Behrend H, Stutz G, Kuster MS. Improvement of primary stability in acl reconstruction by mesh augmentation of an established method of free tendon graft fixation. A biomechanical study on a porcine model. Knee 2013;20:79–84.
[29] Gan RZ, Yang F, Zhang X, Nakmali D. Mechanical properties of stapedial annular ligament. Med Eng Phys 2011;33:330–9.
[30] Sutton MA, Ke X, Lessner SM, Goldbach M, Yost M, Zhao F, et al. Strain field measurements on mouse carotid arteries using microscopic three-dimensional digital image correlation. J Biomed Mater Res A 2008;84:178–90.
[31] Wang S, Bao Y, Guan Y, Zhang C, Liu H, Yang X, et al. Strain distribution of repaired articular cartilage defects by tissue engineering under compression loading. J Orthop Surg Res 2018;13:19.
[32] Zhang D, Arola DD. Applications of digital image correlation to biological tissues. J Biomed Opt 2004;9:691–9.
[33] Kittl C, El-Daou H, Athwal KK, Gupte CM, Weiler A, Williams A, et al. The role of the anterolateral structures and the ACL in controlling laxity of the intact and ACL-deficient knee. Am J Sports Med 2016;44:345–54.
[34] Rahnemai-Azar AA, Miller RM, Guenther D, Fu FH, Lesniak BP, Musahl V, et al. Structural properties of the anterolateral capsule and iliotibial band of the knee. Am J Sports Med 2016;44:892–7.
[35] Vincent JP, Magnussen RA, Gezmez F, Uguen A, Jacobi M, Weppe F, et al. The anterolateral ligament of the human knee: an anatomic and histologic study. Knee Surg Sports Traumatol Arthrosc 2012;20:147–52.